Okhotsk Sea and Polar Oceans Research 1 (2017) 1-6

https://doi.org/10.57287/ospor.1.1

Article

The impact of data assimilation and atmospheric forcing data on predicting short-term sea ice distribution along the Northern sea route

Liyanarachchi Waruna Arampath DE SILVA[1] and Hajime YAMAGUCHI[1]

[1]*The University of Tokyo, Tokyo, Japan*

(Received September 16, 2016; Revised manuscript accepted October 19, 2016)

Abstract

With the recent rapid decrease in summer sea ice in the Arctic Ocean extending the navigation period in the Northern sea routes (NSR), the precise prediction of ice distribution is crucial for safe and efficient navigation in the Arctic Ocean. Precise ice distribution prediction in the short-term (5–days scale) is one of the key issues to realize safe and efficient navigation in the NSR. Ensemble predictions of short-term sea-ice conditions along the Northern sea route have been carried out using a high–resolution (about 2.5km) ice–ocean coupled model that explicitly treats ice floe collisions in marginal ice zones. In this study, the ensembles are constructed by using forecasted atmospheric forcing data sets from THORPEX Interactive Grand Global Ensemble (TIGGE) project in 2015. We also discussed the influence of data assimilation on high-resolution model ice and ocean initial conditions estimated by the whole Arctic medium-resolution (about 25 km) model. The correlation score of ice–edge error and sea ice concentration distribution quantifies forecast skill. Skill scores are computed from 5–days ensemble forecasts initialized in each month between May 2015 to October 2015. Comparison of different ensemble atmospheric forecasts, using different months initial data sets, revealed that our ice–POM numerical model skillfully predicts the ice distribution during the NSR operational period. The average forecast skill of ice–POM model in the melting season is 9.28±2.68 km and in the freezing season without assimilated initial conditions is 15.43±6.29 km and with assimilation 13.85±5.77 km with the 15% thresholds of ice concentration for the ice edge. With data assimilation, there is 10% improvement of average ice edge error within 5-days simulation.

Key words: Arctic sea ice, Data assimilation, Northern sea route

INTRODUCTION

Past decades of satellite observations have shown a rapid decrease of summer Arctic sea ice extent. Furthermore, the Arctic sea ice cover is now thinner, weaker, and drifts faster. Those conditions increase the interest on the commercial use of Arctic shipping. However, the sea ice distribution varies with hourly time scales due to the atmospheric and oceanic conditions. Therefore, sea ice predictions and observations are important to protect the ships and offshore and coastal structures in order to utilize the Northern sea route (NSR). Global climate models have been employed to assess the predictability of Arctic sea ice. However, most of the available numerical models have shown high uncertainties in the short-term (about 5days) and narrow-area predictions, especially marginal ice zones such as the NSR (Hebert *et al.*, 2015). Successful sea ice predictions are relying on comprehensive initial conditions of sea ice variables and ocean variables and an ability of forecast systems to capture high-frequency atmospheric variability and associated feedbacks.

There are 2 kinds of ensemble forecasting systems available for sea ice predictions. First, perturbing the sea ice or ocean initial conditions generates the ensemble members. Second, changing the boundary conditions, such as atmospheric forcing, generates the ensemble members. In this study, the ensembles are constructed by using forecasted atmospheric forcing datasets from THORPEX Interactive Grand Global Ensemble (TIGGE; Bougeault *et al.*, 2010) project in 2015 and the ice and ocean conditions estimated by the hindcast model simulation.

The purpose of this study is to predict the short-term (5days) sea ice conditions in the NSR using mesoscale eddy resolving ice-ocean coupled model within the ice edge error of ±10km, which can meet ship crew requirement. The correlation score of ice edge error and sea ice concentration distribution quantifies forecast skill. Skill scores are computed from 5-days ensemble forecasts initialized in each month between May 2015 to October 2015. Also, we investigate the impact of sea ice predictions by different atmospheric forecasted datasets.

Some researchers suggest that model alone predictions are prone to several errors such as uncertainties in initial conditions, uncertainties in the forcing data and limitations of the temporal and spatial resolutions (Lindsay *et al.*, 2006; Mudunkotuwa *et al.*, 2016). Therefore, in this study, we also investigated the impact of ice and ocean initial conditions into the short-term sea ice predictions by introducing data assimilation into the whole Arctic model.

MODEL DESCRIPTION

Ice–ocean coupled model used in this study is based on the model developed by De Silva *et al.* (2015). The ocean model is based on generalized coordinates, the Message Passing Interface version of the Princeton Ocean Model (POM; Mellor *et al.* (2002)). The level-2.5 turbulence closure scheme of Mellor and Yamada (1982) is used for the vertical eddy viscosity and diffusivity. The horizontal eddy viscosity and diffusivity are calculated using a formula proportional to the horizontal grid size and velocity gradients (Smagorinsky,1963); the proportionality coefficient chosen is 0.2. The ice thermodynamics model is based on the zero-layer thermodynamic model proposed by Semtner (1976). The ice rheological model is based on the elastic–viscous–plastic (EVP) rheology proposed by Hunke and Dukowicz (2002) and is modified to take ice floe collisions into account, following Sagawa and Yamaguchi (2006). Model domain is constructed using Earth Topography one-minute Gridded Elevation Dataset (ETOPO1) as shown in Fig. 1.

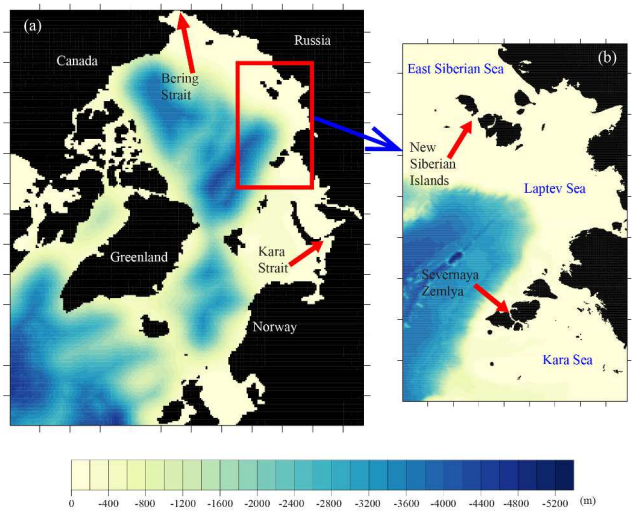

Fig. 1 Model bathymetries (m). (a) Whole-Arctic model.

To avoid the singularity at the North Pole, the whole-Arctic model grid is rotated to place its North Pole over the equator. Red rectangle denotes the high-resolution domain in the Northern Sea Route. (b) High-resolution regional model domain of what in this study we call the Laptev Sea region, consisting of the Laptev Sea and part of the Kara and East Siberian seas, with 50°E - 165°E longitudes and 68°N - 85.5°N latitudes. (De Silva *et al.* 2015)

The zonal and meridional grid spacing are approximately 25 × 25 km for the whole Arctic model and 2.5 × 2.5 km for the high-resolution regional model. To resolve the surface and bottom ocean dynamics, we use the logarithmic distribution of the vertical sigma layers near the top and bottom surfaces.

Mudunkotuwa *et al.* (2016) introduced the data assimilation into the ice-POM model. She claimed that assimilating sea ice variables improved the ocean and ice conditions. It is evident from the changes in sea ice extent, sea ice thickness, and ocean salinity. She also claimed that non-assimilated sea ice variables have also been indirectly improved by assimilation. In this study, we used the Newtonian relaxation (nudging) technique to assimilate the satellite observational (SSMI, AMSR-E, and AMSR2) sea ice concentration in 24hr intervals from year 2000 to 2016. During assimilation experiment, the model estimates concentrations are nudged to new estimate sea ice concentration with the following relationship (Eq.1)

$$A_{\text{new}} = A_{\text{model}} + K\left(A_{\text{obs}} - A_{\text{model}}\right) \quad (1)$$

where, A_{new} newly estimated sea ice concentration, A_{model} model derived sea ice concentration, A_{obs} satellite observational sea ice concentration and K is a weighting constant and this study it set to be 0.8. Some corrections are done to adjust the sea ice thickness, velocity, ocean temperature and salinity while assimilating sea ice concentration. When the assimilation creates ice, the ice thickness and velocity are set to be the average of the four neighboring cells while the maximum thickness of created ice is set to be 0.5m and the minimum is set to 0.1m to avoid immediate melting. When the assimilation removes ice, the values of other sea ice variables (sea-ice thickness and sea-ice velocity) are set to zero. Ocean temperature is also set to freezing temperature if the temperature is below freezing temperature.

High-resolution computations are initialized using interpolated whole-Arctic model results with and without data assimilation (e.g., sea-ice thickness, ocean temperature and salinity). Note that whole-Arctic sea-ice concentration is not used for high-resolution computations; rather, satellite observations Advanced Microwave Radiometer2 (AMSR2) are used. When the initial AMSR2 sea ice concentration is not zero in the open water areas of the whole-Arctic simulation, we interpolated the sea-ice thickness from neighboring grid cells. In this case, water surface temperature under those cells was set to the freezing temperature to avoid the rapid melting of sea ice. Moreover, when the initial AMSR2 observed concentration is zero and the whole-Arctic simulation concentration is not zero, we set the sea-ice thickness to zero in those cells. For those

cells, the temperature under the ocean surface was assigned by interpolating the values only from the open water neighboring grid cells. Note that, in both situations, ocean salinity is unchanged and the same as the interpolated whole-Arctic model output value. In the marginal regions (open boundaries) of the high-resolution model, the whole-Arctic model results interpolated into the high-resolution model grids are applied for both the sea-ice and ocean open-boundary conditions with daily intervals.

The atmospheric dataset used in this ensemble forecast study comes from TIGGE (Bougeault *et al.*, 2010) operational medium-range ensemble forecast project. The operational ensemble prediction systems used in this study include the China Metrological Administration (CMA), the Canadian Metrological center (CMC), the European Center for Medium-range Weather Forecasts (ECMWF), the Japan Metrological Agency (JMA), the France Metrological Office (FMO), the United Kingdom Meteorological Office (UKMO), and the US National Centers for Environmental Prediction (NCEP). The more details about the atmospheric forecasting and reanalysis are described in Bougeault *et al.* (2010). We used the 6-hourly atmospheric data outputs with the spatial resolution of 0.5-degree; air-temperature and dev-point temperature at 2m height, wind at 10m height, precipitation, sea-level pressure, and cloud cover. Using these data, surface fluxes, shortwave radiation, longwave radiation, sensible heat flux and latent heat flux are calculated according to the bulk formulation proposed by Parkinson and Washington (1979).

DISCUSSION

To evaluate the sea ice predictions using different atmospheric datasets, we used the correlation score of ice edge error and sea ice concentration distribution. The ice edge error is defined as follows (Eq. 2). First, the difference in the ice areas between the model's predictions and AMSR2 satellite observations are calculated, shown in Fig. 2. Note that area covered with ice concentration more than 15%, 30%, and 50% are taken into comparison. Because the definition of the opening of sea route highly depends on the ice level of an icebreaker. Next, dividing the length of the model predicted contour of the ice concentration of 15%, 30%, and 50%, we obtain the ice edge error with the dimension of length.

$$\text{ice edge error} = \frac{\text{Area enclosed by both contours}}{\text{Length of model predicted ice edge}} \qquad (2)$$

The results of the 5days in melting season (20 to 25 July 2015) forecasted ice edge errors and the hindcast ice edge error using ERA-Interim data are shown in Fig. 3. Ocean and ice initial conditions are initialized using the whole Arctic model alone run. There were no significant differences of ice edge errors between different forecasted datasets and ERA-interim hindcast data. Within 5 days, average ice edge errors among seven-forecasted datasets are 9.28±2.68 km, 10.11±3.08 km, 10.04±3.51 km with respect to the threshold value of ice concentration 15%, 30%, and 50% respectively. There is a slight increment in the average ice edge error when the threshold values of ice concentration increase from 15% to 50%.

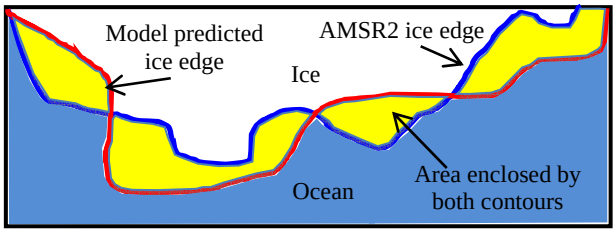

Fig. 2 Schematic diagram of model predicted (red) and AMSR2 (blue) observational ice edges and area enclosed by both contours (yellow)

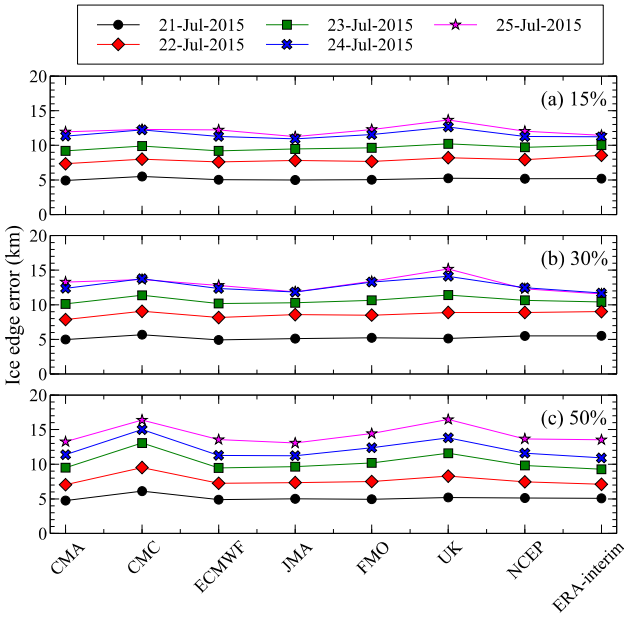

Fig. 3 Ice edge error between different forecasted datasets (and ERA-interim) and AMSR2 observations from 21-July-2015 to 25-July-2015 Top threshold value of ice concentration (a) 15% (b) 30% and (c) 50%

During the computation period, the JMA showed best ice edge error prediction of 8.89±2.57 km. Overall, in melting season ice-POM model reproduced the ice edge error within the limit of 10km.

In addition to the quantitative comparisons of ice edge error, we compared the sea-ice concentration distribution qualitatively. Fig. 4 shows the difference between the model and AMSR2 sea ice concentrations after the 5th day of computation (25 July 2015). In the western part of the domain (Kara sea), the difference in sea ice concentration is higher compared to the other

regions. This discrepancy could be due to the underestimation of heat transfer process between ice and ocean. However, sea ice spatial distribution between different datasets has no significant differences in the melting season.

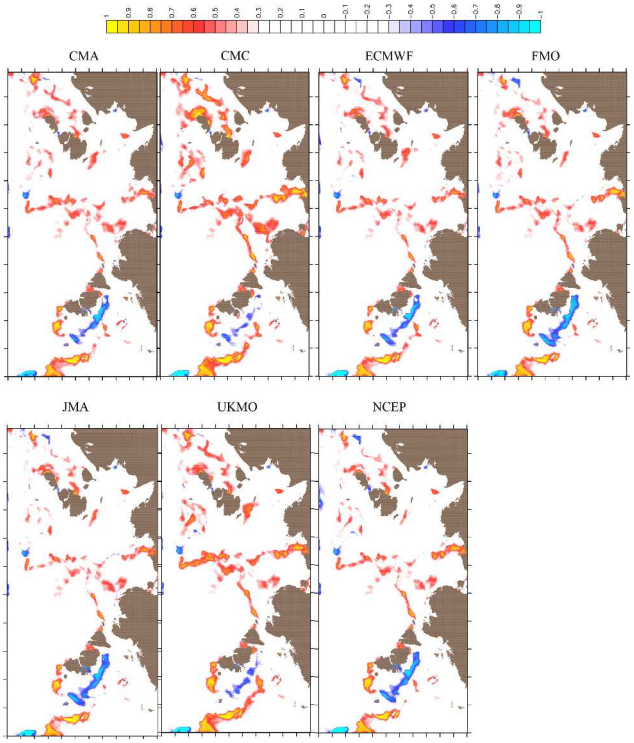

Fig. 4 Sea ice concentration distribution, Difference between model-predicted ice concentration and AMSR2 observation on 25-July-2015. Threshold value of ice concentration is 15%

Next, the results of the 5days in the period of Arctic annual minimum sea ice extent (10 to 15 September 2015) forecasted ice edge error and the hindcast ice edge error using ERA-Interim data is shown in Fig. 5. Except for CMA dataset there were no significant differences of ice edge error between different forecasted datasets. The average ice edge errors with respect to the different ice concentration threshold values are 15% threshold value 10.15±3.45 km, 30% threshold value 10.56±2.8 km and 50% threshold value 12.87±2.15 km. There is a slight increment in the average ice edge error when the threshold values of ice concentration increase from 15% to 50%.

Finally, the results of the 5days in freezing season (10 to 15 October 2015) forecasted ice edge error and the hindcast ice edge error using ERA-Interim data is shown in Fig. 6. There were significant differences of ice edge error between different forecasted datasets and ERA-interim hindcast data after the 2nd day (12- Oct. 2015) of computation. The average ice edge errors with respect to the different ice concentration threshold values are 15% threshold value 15.43±6.29 km, 30% threshold value 16.56±7.08 km and 50% threshold value 19.76±8.98 km. There is a significant increment in the average ice edge error when the threshold values of ice concentration increase from 15% to 50%.

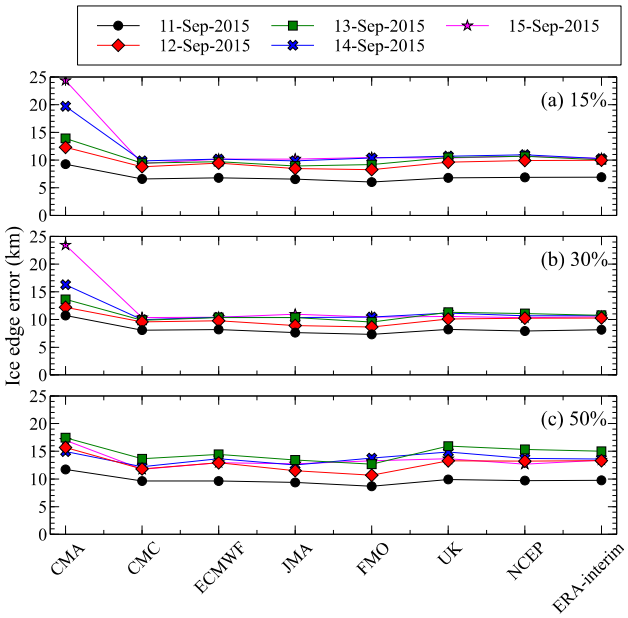

Fig. 5 Ice edge error between different forecasted datasets (and ERA-interim) and AMSR2 observations from 11-Sep-2015 to 15-Sep-2015 (a) threshold value of ice concentration 15% (b) 30% and (c) 50%

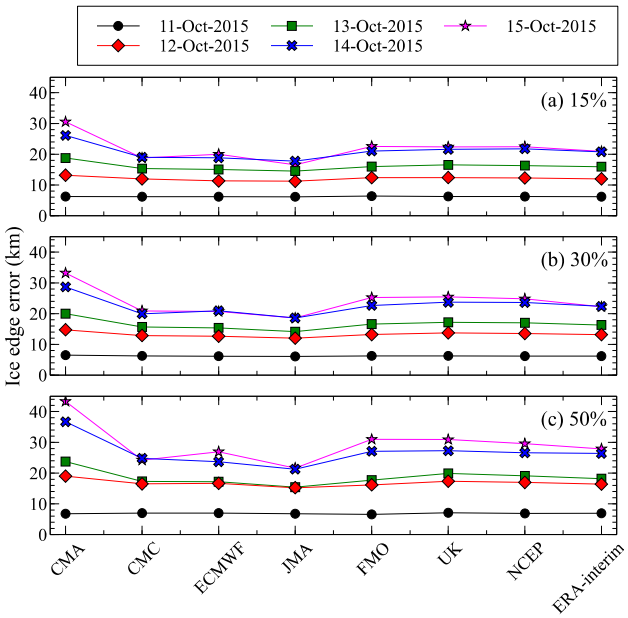

Fig. 6 Ice edge error between different forecasted datasets (and ERA-interim) and AMSR2 observations from 11-Oct-2015 to 15-Oct-2015 (a) threshold value of ice concentration 15% (b) 30% and (c) 50%

In most cases, the average ice edge error increases with the threshold values of ice concentration increase

from 15% to 50%. We speculate the reason for this issue as follows. In practice, the regions where ice concentration change from 15% to 50% are usually very narrow and subjected to the observational errors due to melt ponds and surface conditions of snow cover in melting and early freezing seasons. These issues might favorably affect the ice edged error calculations in less ice concentration areas.

It is also seen that time evolution of ice edge error is significantly large in the freezing season compared to the melting season and annual minimum ice extent. We believe this discrepancy could be due to the uncertainties in the model initial conditions.

The lower ice edge error values in the summer suggest ice-POM does a good job at capturing ice melt, while higher values during the freezing season suggest that ice-POM not produce ice as fast as actually occurs along the NSR.

Several possibilities exist to explain these discrepancies. The first reason could be because we used the bulk formulation proposed by Parkinson and Washington (1979) to produce the heat fluxes from the atmosphere to sea ice and those parameters may not have tuned into the latest Arctic conditions properly. The second reason could be coarseness of spatial and temporal resolution of forecasted datasets could not properly resolve the small-scale features of the atmosphere (Ono *et al.* 2016), which influenced the sea ice production and retrieve. These will be the topic of future study.

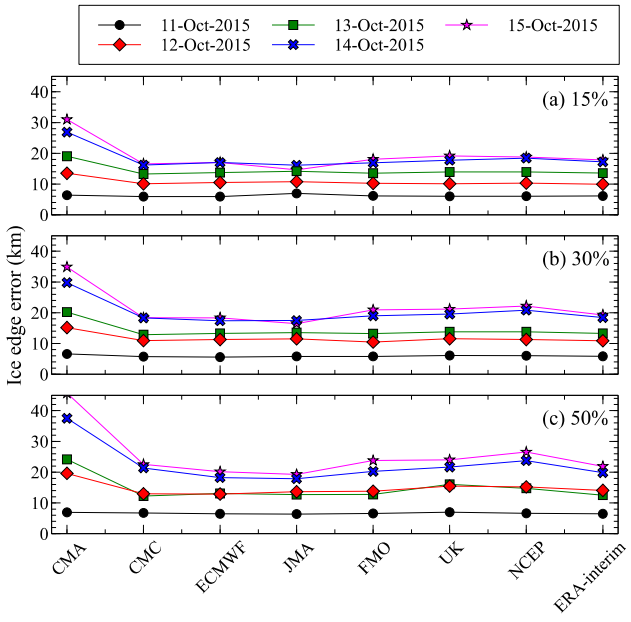

Fig. 7 Same as Fig. 6 but model initialized from whole Arctic model with assimilation results

The third reason could be because we used ocean temperature and salinity data from the interpolated whole-Arctic model for our high-resolution computations as an initial condition. Over prediction of ocean surface heat in the whole-Arctic model delayed the freezing of sea ice in the high-resolution models freezing season.

We have tested the third hypothesis in this study. We have run the whole Arctic model with data assimilation from year 2000 to 2016 and used the assimilated whole Arctic model data for high-resolution initial conditions.

The results of the 5days in freezing season (10 to 15 October 2015), initialized with data assimilated results, forecasted ice edge error and the hindcast ice edge error using ERA-Interim data is shown in Fig. 7. The average ice edge errors with respect to the different ice concentration threshold values are 15% threshold value 13.85±5.77 km, 30% threshold value 14.84±6.78 km and 50% threshold value 17.12±8.61 km. Compared with the model alone initialized computation there is 10% ice edge error improvement can be seen.

Fig. 8 shows the ocean temperature difference between data assimilated results and model alone results in the Laptev Sea on 10th October 2015. It's very clear that along the ice edge (Fig. 8 black contours) less heat in the data assimilated model compared to the model alone.

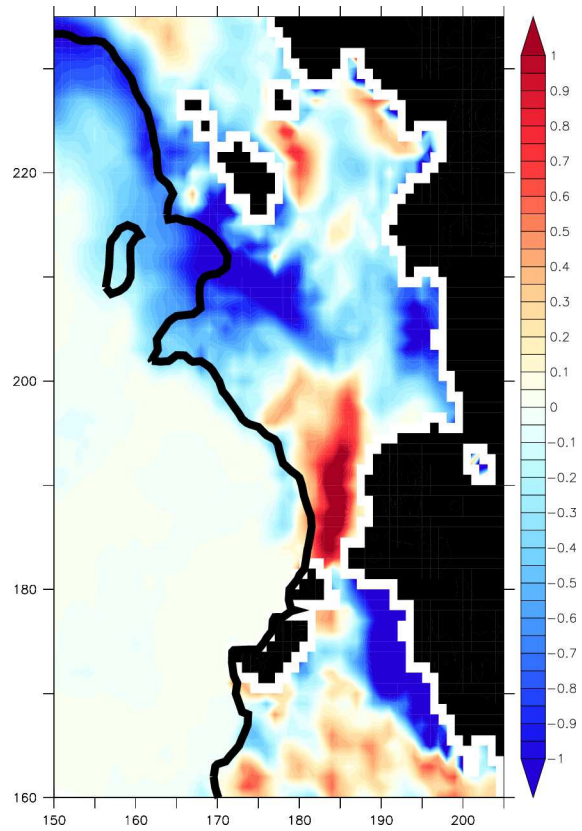

Fig. 8 Ocean temperature difference (degree) between data assimilated model run and model alone run in the Laptev Sea region on 10-October-2015 (freezing season initial date). Black contour shows the AMSR2 sea ice edge (concentration threshold 15%)

CONCLUSION

Sea ice forecasted skill of different dataset (TIGGE) is evaluated in the study. The average forecast skill of ice-POM model in the melting season is 9.28±2.68 km that is in good agreement with the requirement of an operational ice navigation system (10 km). Also, there is good forecast skill (10.15±3.45 km) in the ice-POM model when the Arctic sea ice extent hits its annual minimum. However, in the freezing season ice edge error become 15.43±6.29 km. But after introducing the data assimilation into the whole Arctic model freezing season ice edge error improved 10% from without assimilated results. However, to improve the model forecast accuracy, the further studies would be necessary for the freezing season.

ACKNOWLEDGEMENTS

The authors wish to acknowledge support from the Green Network of Excellence Program Arctic Climate Change Research Project (GRENE) and Arctic Challenge for Sustainability Research Project (ArCS) by the Japanese Ministry of Education, Culture, Sports, Science and Technology and a Kakenhi grant (no. 26249133) from the Japan Society for the Promotion of Science. We also thank Ms. Dulini Yasara Mudunkotuwa for her useful comments. Their gratitude is extended to The National Snow and Ice Data Center for the gridded AMSR-2 data, Arctic Data Archive System (ADS) for providing sea ice thickness gridded data.

REFERENCES

Bougeault, P. and 21 others (2010): The THORPEX Interactive Grand Global Ensemble. *Bull. Am. Meteorol. Soc.*, **91**, 1059–1072.

De Silva, L. W. A., H. Yamaguchi, and J. Ono (2015): Ice–ocean coupled computations for sea-ice prediction to support ice navigation in Arctic sea routes. *Polar Res.*, **34**, 18pp.

Hebert, D. A., R. A. Allard, E. J. Metzger, P. G. Posey, R. H. Preller, A. J. Wallcraft, M. W. Phelps, and O. M. Smedstad (2015): Short-term sea ice forecasting: An assessment of ice concentration and ice drift forecasts using the U.S. Navy's Arctic Cap Nowcast/Forecast System. *J. Geophys. Res. Ocean.*, **120**, 8327–8345.

Hunke, E. C., and J. K. Dukowicz (2002): The elastic-viscous-plastic sea ice dynamics model in general orthogonal curvilinear coordinates on a sphere-incorporation of metric terms. *Mon. Weather Rev.*, 1848–1865.

Lindsay, R. W., J. Zhang, R. W. Lindsay, and J. Zhang (2006): Assimilation of Ice Concentration in an Ice–Ocean Model. *J. Atmos. Ocean. Technol.*, **23**, 742–749.

Mellor, G. L., and T. Yamada (1982): Development of a turbulence closure model for geophysical fluid problems. *Rev. Geophys.*, **20**, 851–875.

Mellor, G. L., S. Hakkinen, T. Ezer, and R. Patchen (2002): A generalization of a sigma coordinate ocean model and an intercomparison of model vertical grids. *In Ocean Forecasting: Conceptual Basis and Applications.*, Springer, Berlin Heidelberg, 55–72.

Mudunkotuwa, D. Y., L. W. A. De Silva, and H. Yamaguchi (2016): Data assimilation system to improve sea ice predictions in the Arctic Ocean using an ice-ocean coupled model. *23rd IAHR International Symposium on Ice*, Ann Arbor, Michigan USA, 1-8.

Ono, J., J. Inoue, A. Yamazaki, K. Dethloff, and H. Yamaguchi (2016): The impact of radiosonde data on forecasting sea-ice distribution along the Northern Sea Route during an extremely developed cyclone. *J. Adv. Model. Earth Syst.*, **8**, 292–303.

Parkinson, C. L., and W. M. Washington (1979): A large-scale numerical model of sea ice. *J. Geophys. Res.*, **84**, 311–337

Sagawa, G., and H. Yamaguchi (2006): A Semi-Lagrangian Sea Ice Model For High Resolution Simulation. *The Sixteenth International Offshore and Polar Engineering Conference*, San Francisco, California, International Society of Offshore and Polar Engineers, 584–590.

Semtner, A. J. (1976): A Model for the Thermodynamic Growth of Sea Ice in Numerical Investigations of Climate. *J. Phys. Oceanogr.*, **6**, 379–389.

Smagorinsky, J. (1963): General circulation experiments with the primitive equations. *Mon. Weather Rev.*, **91**, 99–164.